Numerical Analysis of Arbitrarily Shaped Discontinuities Between Planar Dielectric Waveguides with Different Thicknesses

KOICHI HIRAYAMA, MEMBER, IEEE, AND MASANORI KOSHIBA, SENIOR MEMBER, IEEE

Abstract — **An approach that combines the finite-element and boundary-element methods is applied to the analysis of arbitrarily shaped discontinuities between planar dielectric waveguides with different thicknesses. The fields interior and exterior to the region enclosing the discontinuities are treated by the finite-element and the boundary-element method, respectively. The waveguide regions connected to the discontinuities are handled by analytical solutions. In this approach, scattering characteristics of the discontinuities can be accurately evaluated, and far-field radiation patterns can be easily calculated. To show the validity and usefulness of this approach, the scattering characteristics of a step, a staircase transformer, and a tapered transformer are analyzed. Also, a simple equivalent network approach is introduced for estimating the reflection and transmission characteristics of planar dielectric waveguide discontinuities, and the effectiveness of this simple approach is confirmed by comparing the numerical results with those of the approach that combines the finite-element and boundary-element methods.**

I. Introduction

DISCONTINUITIES in planar dielectric waveguides play an important role in millimeter-wave, submillimeter-wave, and optical systems. Various theoretical approaches have therefore been developed for the problem of planar dielectric waveguide discontinuities. Recently, the integral equation method (IEM) [1]–[4], the boundary-element method (BEM) [5], the finite-element method (FEM) [6], and a combination of the finite-element and boundary-element methods (CFBEM) [7] have been presented for the analysis of discontinuities with arbitrarily shaped boundaries. In [1]–[4] using the IEM, however, only the weakly guiding structure is considered. Also, the BEM cannot be effectively applied to the problem of inhomogeneous discontinuities [5]. The FEM and CFBEM are very useful for arbitrarily shaped and inhomogeneous discontinuities. In [6] using the FEM, however, the evaluation of radiation patterns seems to be difficult since the normalized radiated power P_r is estimated by the relation $P_r = 1 - |R_0|^2 - |T_0|^2$, where R_0 and T_0 are, respectively, the reflection and transmission coefficients of the fundamental guided mode. The CFBEM may be useful for the evaluation of scattering characteristics including radiation patterns. In [7] using the CFBEM, however, a method of evaluating the radiation patterns is not shown, and only the discontinuities in a uniform planar dielectric waveguide are analyzed.

Manuscript received May 30, 1989; revised October 20, 1989.

K. Hirayama is with the Department of Electronic Engineering, Kushiro National College of Technology, Kushiro, 084 Japan.

M. Koshiba is with the Department of Electronic Engineering, Hokkaido University, Sapporo, 060 Japan.

IEEE Log Number 8932996.

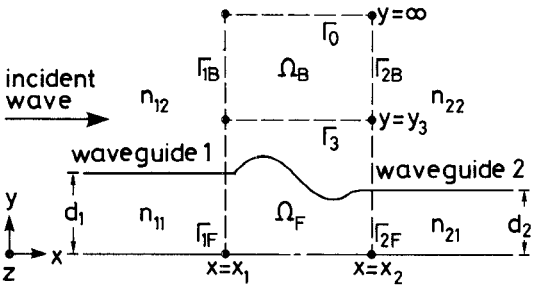

Fig. 1. Geometry of the problem.

In this paper, the CFBEM is applied to the analysis of discontinuities between planar waveguides with different thicknesses. The scattering characteristics of a step, a staircase transformer, and a tapered transformer are analyzed, and the normalized reflection, transmission, and radiated powers, as well as the radiation patterns for these discontinuities, are presented. The accuracy of the CFBEM is checked by comparing the numerical results with those of the well-known Rozzi method [8]. Also, a simple equivalent network approach is introduced for estimating the reflection and transmission coefficients of planar dielectric waveguide discontinuities. The effectiveness of this simple approach is confirmed by comparing the results of the equivalent network method with those of the CFBEM.

II. Mathematical Formulation

Consider the symmetric (relative to $y = 0$) mode excitation of the symmetric planar dielectric waveguide shown in Fig. 1. The boundary Γ_0 is placed at infinity ($y = \infty$) and the boundary $\Gamma_i = \Gamma_{iF} + \Gamma_{iB}$ ($i = 1, 2$) connects the discontinuity region $x_1 \leqslant x \leqslant x_2$ to the uniform waveguide i, where d_i and n_{ij} ($j = 1, 2$) are the half-thickness and the refractive index of the waveguide i ($n_{i1} > n_{i2}$), respectively. The region Ω_F surrounded by the boundary $\Gamma_F = \Gamma_{1F} + \Gamma_{2F} + \Gamma_3$

0018-9480/90/0300-0260$01.00 ©1990 IEEE

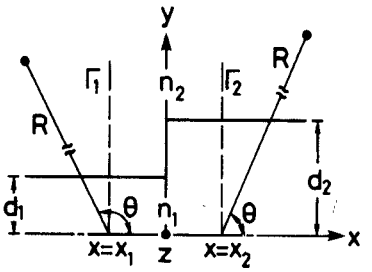

Fig. 2. Step discontinuity ($n_1=\sqrt{5}$, $n_2=1$, $d_1=\lambda/10\pi$, and $d_2=\lambda/2\pi$).

and the symmetry plane ($y=0$) completely encloses the discontinuity region, and the region Ω_B is surrounded by the boundaries $\Gamma_B=\Gamma_{1B}+\Gamma_{2B}+\Gamma_3$ and Γ_0.

We assume that there is no variation in the z direction and that the fundamental mode ($m=0$) of unit amplitude is incident from the left side of waveguide 1 in Fig. 1.

Applying the FEM with six-node triangular elements and the BEM with three-node line elements to Ω_F and Ω_B, respectively, and introducing the analytical solutions in waveguides 1 and 2, we obtain the following final matrix equation [7]:

$$\left(\begin{array}{c|c} [A'] & -[B'] \\ [H'] & -[G'] \\ \hline [1][0][0] & -[Z]_1[0][0] \\ [0][1][0] & [0]-[Z]_2[0] \end{array}\right)\left(\begin{array}{c} \{\phi\}_1 \\ \{\phi\}_2 \\ \{\phi\}_3 \\ \hline \{\psi\}_1 \\ \{\psi\}_2 \\ \{\psi\}_3 \end{array}\right)=\left(\begin{array}{c} \{0\} \\ \{0\} \\ \hline \{f\}_1 \\ \{0\} \end{array}\right). \quad (1)$$

The components of the vectors $\{\phi\}_i$ and $\{\psi\}_i$ ($i=1,2,3$) are the values of ϕ and ψ at the nodes on Γ_i, respectively, where

$$\phi = Ez \quad \text{for TE modes} \quad (2a)$$

$$\phi = Hz \quad \text{for TM modes} \quad (2b)$$

and

$$\psi = -\lambda\,\partial\phi/\partial x \quad \text{on } \Gamma_1 \quad (3a)$$

$$\psi = \lambda\,\partial\phi/\partial x \quad \text{on } \Gamma_2 \quad (3b)$$

$$\psi = -\lambda\,\partial\phi/\partial y \quad \text{on } \Gamma_3. \quad (3c)$$

Here λ is the free-space wavelength. The matrices $[A']$ and $[B']$ are generated by the FEM, the matrices $[H']$ and $[G']$ are generated by the BEM, and the matrix $[Z]_i$ ($i=1,2$) is obtained from the analytical approach for the waveguide i. Also, the vector $\{f\}_1$ describes the incident wave, $\{0\}$ is a null vector, [0] is a null matrix, and [1] is a unit matrix.

The solutions of (1) allow the determination of the normalized reflection power $|R_m|^2$ and normalized transmission power $|T_m|^2$ of the mth mode, and the normalized radiated power P_r [7]. Also, setting $x-x_i=R\cos\theta$ ($i=1,2$) and $y=R\sin\theta$ (x_i, R, and θ are shown in Fig. 2, where $\pi/2<\theta<\pi$ in waveguide 1 and $0<\theta<\pi/2$ in waveguide 2) and using the saddle point method under the assumption of $R\gg\lambda$, we can evaluate the far-field radiation pattern as follows:

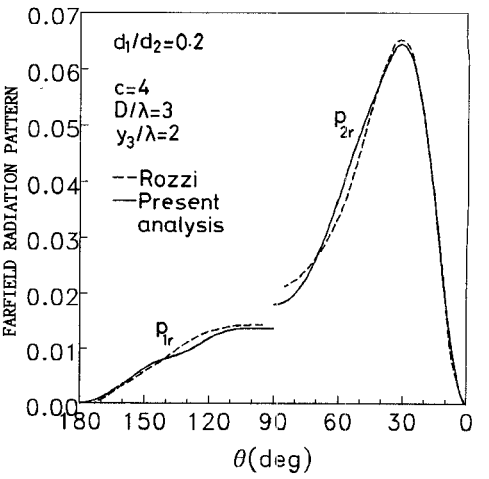

Fig. 3. Far-field radiation pattern of the step.

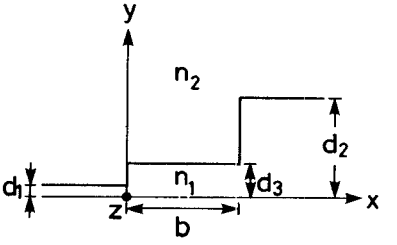

Fig. 4. Staircase transformer ($n_1=\sqrt{5}$, $n_2=1$, $d_1=\lambda/20\pi$, $d_2=\lambda/2\pi$, and $d_3=\lambda/6\pi$).

$$p_{ir}(\theta) \sim \left|\{\hat{g}(\rho_0)\}_i^T\{\psi\}_i\right|^2/(\beta_{10}\lambda^2) \quad (4a)$$

$$\rho_0 = \mp n_{i2}k_0\sin\theta \quad (4b)$$

$$k_0 = 2\pi/\lambda. \quad (4c)$$

Here β_{10} is the phase constant of the fundamental mode in waveguide 1; the double signs $-$ and $+$ are for $i=1$ and 2, respectively; the superscript T denotes a transpose; and the vector $\{\hat{g}(\rho)\}_i$ is the same as (9d) in [7].

III. Computed Results

The convergence of the solutions of the CFBEM has been discussed in detail in [7] and is omitted here. To save space, only the results of the fundamental TE mode are shown in this section.

First, we consider the step shown in Fig. 2. The normalized reflection, transmission, and radiated powers of the step have been given in [7].

Fig. 3 shows the radiation pattern. The parameters c, D, and y_3 are defined in [7]. Our results agree well with those of Rozzi [8]. Comparing our results (Fig. 3 in the present paper and fig. 7 in [7]) with those of Rozzi [8, figs. 4 to 6], it is confirmed that, using the CFBEM, we may evaluate the scattering characteristics including the radiation pattern with good accuracy.

Next, we consider the staircase transformer shown in Fig. 4.

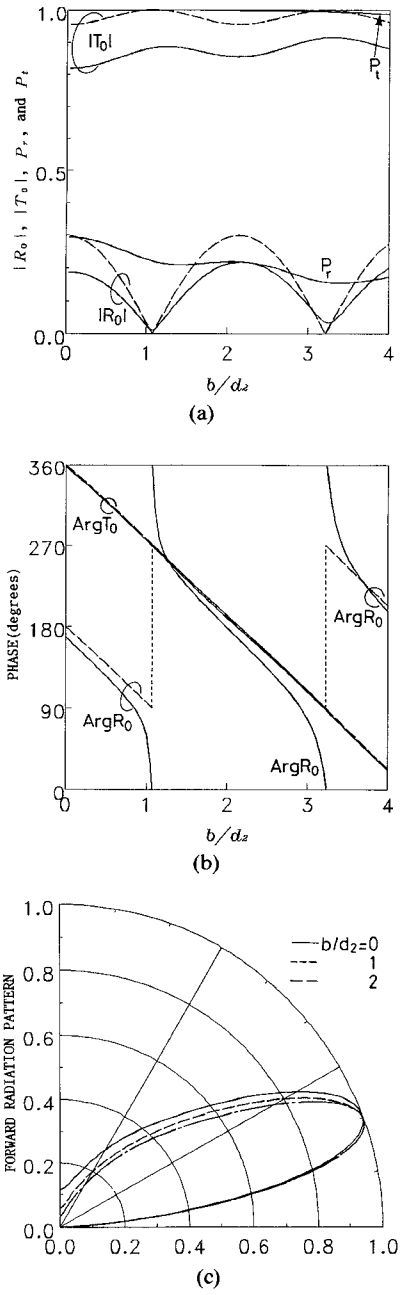

Fig. 5. Scattering characteristics of the staircase transformer ($c=4$, $D/\lambda=3$, and $y_3/\lambda=2$).

Fig. 5 shows the scattering characteristics for the case where the fundamental TE mode is incident from the left side of waveguide 1. Here, the solid lines in parts (a) and (b) of Fig. 5 represent the results of the CFBEM, P_t is the total power, namely $P_t=|R_0|^2+|T_0|^2+P_r$, and Fig. 5(c) shows the forward radiation pattern, i.e., $p_{2r}(\theta)$. The reference planes in Fig. 4 for evaluating the phases of the reflection and transmission coefficients are, respectively, $x=0$ and $x=b$.

The staircase transformer is designed so as to satisfy $\beta_{30}^2 \simeq \beta_{10}\beta_{20}$, where β_{10}, β_{20}, and β_{30} are the phase constants of the fundamental TE mode in waveguide 1, waveguide 2, and the middle waveguide, respectively. Hence, when $\beta_{30}b=l\pi/2$, that is, $b/d_2=l\pi/2\beta_{30}d_2 \simeq 1.08\times l$ ($l=1,3,5,\cdots$), the impedance matching condition is

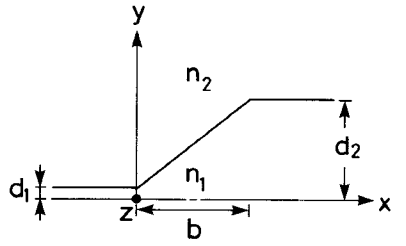

Fig. 6. Tapered transformer ($n_1=\sqrt{5}$, $n_2=1$, $d_1=\lambda/20\pi$, and $d_2=\lambda/2\pi$).

achieved. In fact, we observe in Fig. 5(a) that the magnitudes of the reflection coefficient reach a minimum near $b/d_2=1.08$ and 3.25. Also, we find in Fig. 5(c) that the main lobe of the radiation pattern is in the direction of 20°.

Finally, we consider the tapered transformer shown in Fig. 6.

Fig. 7 shows the scattering characteristics for the case where the fundamental TE mode is incident from the left side of waveguide 1. As the value of b increases, that is, as the taper configuration becomes gentler, the magnitudes of the reflection coefficient are smaller, but there is a significant amount of radiation, 20 to 30 percent, all over the range of $0 \leqslant b/d_2 \leqslant 4$. We note that the behavior of the phase of the reflection coefficient in Fig. 7 differs significantly from that in Fig. 5.

Now we consider the simple equivalent network shown in Fig. 8 for the staircase transformer in Fig. 4. Here, Z_t is the characteristic impedance for TE modes and is given by $\omega\mu_0/\beta_{t0}$, where ω is the angular frequency and μ_0 is the permeability of free space. Using the impedance matching condition $Z_3^2=Z_1Z_2$, from the equivalent network in Fig. 8 the normalized reflection and transmission coefficients are given as follows:

$$R_0=\frac{(Z_2-Z_1)\cos(\beta_{30}b)}{(Z_1+Z_2)\cos(\beta_{30}b)+j2\sqrt{Z_1Z_2}\sin(\beta_{30}b)} \tag{5a}$$

$$T_0=\frac{2\sqrt{Z_1Z_2}}{(Z_1+Z_2)\cos(\beta_{30}b)+j2\sqrt{Z_1Z_2}\sin(\beta_{30}b)}. \tag{5b}$$

The sum of $|R_0|^2$ and $|T_0|^2$ always equals 1, and the radiation loss is not taken into account at all.

The broken lines in parts (a) and (b) of Fig. 5 represent the results of (5), where the dotted lines show the discontinuous change of the phase by 180°.

On the other hand, since we cannot replace the tapered transformer in Fig. 6 by the equivalent network directly, we subdivide the tapered region into a number of uniform waveguides with the same length and consider the equivalent network shown in Fig. 9. The normalized reflection and transmission coefficients are given by

$$R_0=\frac{AZ_2+B-CZ_1Z_2-DZ_1}{AZ_2+B+CZ_1Z_2+DZ_1} \tag{6a}$$

$$T_0=\frac{2\sqrt{Z_1Z_2}}{AZ_2+B+CZ_1Z_2+DZ_1}. \tag{6b}$$

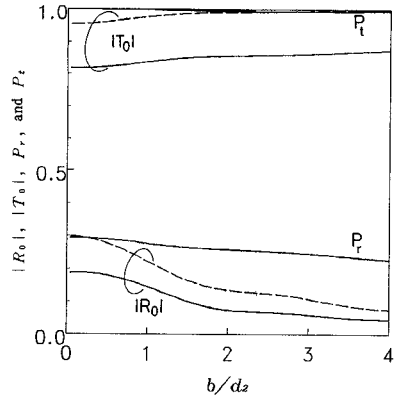

(a)

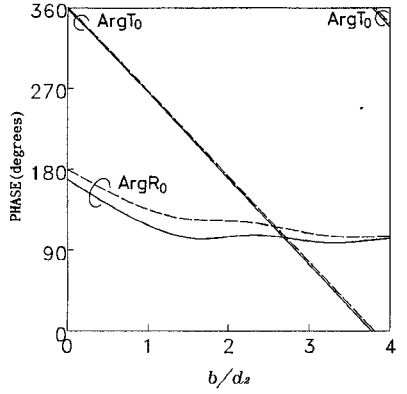

(b)

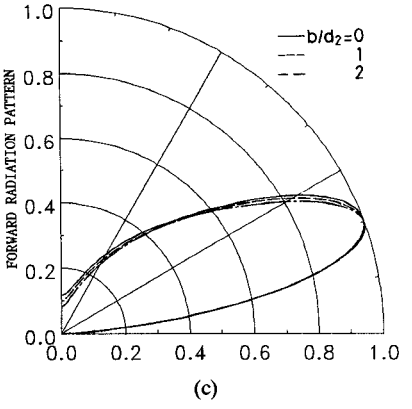

(c)

Fig. 7. Scattering characteristics of the tapered transformer ($c=4$, $D/\lambda=3$, and $y_3/\lambda=2$).

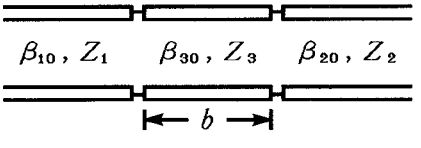

Fig. 8. Equivalent network for the staircase transformer.

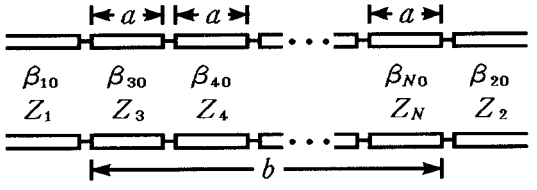

Fig. 9. Equivalent network for the tapered transformer ($a=b/(N-2)$).

A, B, C, and D are expressed as

$$\begin{pmatrix} A & B \\ C & D \end{pmatrix} = [F_3][F_4]\cdots[F_N] \tag{7}$$

where

$$[F_i] = \begin{pmatrix} \cos(\beta_{t0}a) & jZ_t\sin(\beta_{t0}a) \\ (j/Z_t)\sin(\beta_{t0}a) & \cos(\beta_{t0}a) \end{pmatrix}, \quad a = b/(N-2). \tag{8}$$

The broken lines in parts (a) and (b) of Fig. 7 represent the results of (6) with $N=12$ ($N-2=10$).

It is found from Figs. 5 and 7 that in the magnitudes of the reflection and transmission coefficients, the solid and broken lines behave quite similarly, but differ in the values themselves since no radiation loss is taken into account in the equivalent network model.

In the phases of the transmission coefficient in Fig. 5, the results of the equivalent network approach are in excellent agreement with those of the CFBEM. On the other hand, in the phases of the reflection coefficient in Fig. 5, the results of the CFBEM vary gradually while those of the equivalent network approach change discontinuously.

From a physical point of view, the phases of the reflection coefficient for the case $b=0$, namely, a step, should be somewhat shifted from just 180° or 360°, as represented by the solid lines. This phase shift is not taken into account in the equivalent network model.

It is confirmed from Figs. 5 and 7 that the equivalent network approach is very useful for estimating the reflection and transmission characteristics of planar dielectric waveguide discontinuities.

IV. Conclusions

Discontinuities between planar dielectric waveguides with different thicknesses were analyzed by using the CFBEM. First we calculated the far-field radiation pattern for a step and confirmed that, in the CFBEM, the scattering characteristics including the radiation pattern can be accurately evaluated. Next we computed the scattering characteristics for a staircase transformer and a tapered transformer by using the CFBEM and the simple equivalent network approach. It was found that the equivalent network model is very useful for estimating the reflection and transmission characteristics of planar dielectric waveguide discontinuities.

We intend to extend the CFBEM to discontinuities in an asymmetric planar dielectric waveguide and to improve the equivalent network method for more precise discussions in the future.

References

[1] N. Morita, "An integral equation method for electromagnetic scattering of guided modes by boundary deformations of dielectric slab waveguides," *Radio Sci.*, vol. 18, pp. 39–47, Jan.–Feb. 1983.

[2] T. Nobuyoshi, N. Morita, and N. Kumagai, "Analysis of the optical waveguide junctions by means of integral equation method," (in Japanese) *Trans. Inst. Electron. Commun. Eng. Japan*, vol. J66-C, pp. 828–834, Nov. 1983.

[3] E. Nishimura, N. Morita, and N. Kumagai, "Theoretical investigation of a gap coupling of two dielectric slab waveguides with

arbitrarily shaped ends," (in Japanese) *Trans. Inst. Electron. Commun. Eng. Japan*, vol. J67-C, pp. 714–721, Oct. 1984.
[4] E. Nishimura, N. Morita, and N. Kumagai, "An integral equation approach to electromagnetic scattering from arbitrarily shaped junctions between multilayered dielectric planar waveguides," *J. Lightwave Technol.*, vol. LT-3, pp. 887–894, Aug. 1985.
[5] M. Koshiba and M. Suzuki, "Boundary-element analysis of dielectric slab waveguide discontinuities," *Appl. Opt.*, vol. 25, pp. 828–829, Mar. 1986.
[6] S.-J. Chung and C. H. Chen, "A partial variational approach for arbitrary discontinuities in planar dielectric waveguides," *IEEE Trans. Microwave Theory Tech.*, vol. 37, pp. 208–214, Jan. 1989.
[7] K. Hirayama and M. Koshiba, "Analysis of discontinuities in an open dielectric slab waveguide by combination of finite and boundary elements," *IEEE Trans. Microwave Theory Tech.*, vol. 37, pp. 761–768, Apr. 1989.
[8] T. E. Rozzi, "Rigorous analysis of the step discontinuity in a planar dielectric waveguide," *IEEE Trans. Microwave Theory Tech.*, vol. MTT-26, pp. 738–746, Oct. 1978.

✠

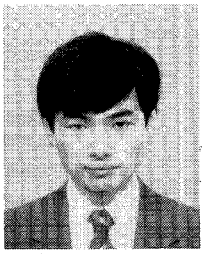

Koichi Hirayama (M'89) was born in Shiranuka, Hokkaido, Japan, on September 8, 1961. He received the B.S., M.S., and Ph.D. degrees in electronic engineering from Hokkaido University, Sapporo, Japan, in 1984, 1986, and 1989, respectively.

In 1989, he joined the Department of Electronic Engineering, Kushiro National College of Technology, Kushiro, Japan. He has been interested in the analysis of discontinuity problems in open dielectric waveguides.

Dr. Hirayama is a member of the Institute of Electronics, Information and Communication Engineers (IEICE).

✠

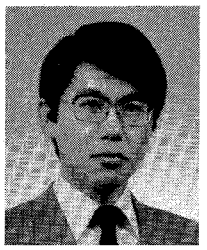

Masanori Koshiba (SM'84) was born in Sapporo, Japan, on November 23, 1948. He received the B.S., M.S., and Ph.D. degrees in electronic engineering from Hokkaido University, Sapporo, Japan, in 1971, 1973, and 1976, respectively.

In 1976, he joined the Department of Electronic Engineering, Kitami Institute of Technology, Kitami, Japan. From 1979 to 1987, he was an Associate Professor of Electronic Engineering at Hokkaido University, and in 1987 he became a Professor. He has been engaged in research on lightwave technology, surface acoustic waves, magnetostatic waves, microwave field theory, and applications of finite-element and boundary-element methods to field problems.

Dr. Koshiba is a member of the Institute of Electronics, Information and Communication Engineers (IEICE), the Institute of Television Engineers of Japan, the Institute of Electrical Engineers of Japan, the Japan Society for Simulation Technology, and the Japan Society for Computational Methods in Engineering. In 1987, he was awarded the 1986 Paper Award by the IEICE.